PROCEEDINGS B

rspb.royalsocietypublishing.org

Research

Cite this article: Palmer-Young EC, Raffel TR, McFrederick QS. 2018 Temperature-mediated inhibition of a bumblebee parasite by an intestinal symbiont. *Proc. R. Soc. B* **285**: 20182041.
http://dx.doi.org/10.1098/rspb.2018.2041

Received: 9 September 2018
Accepted: 9 October 2018

Subject Category:
Ecology

Subject Areas:
ecology, microbiology, health and disease and epidemiology

Keywords:
thermal performance asymmetry, temperature-mediated competition, gut microbiome, *Bombus*, *Crithidia*, *Lactobacillus bombicola*

Author for correspondence:
Evan C. Palmer-Young
e-mail: ecp52@cornell.edu

Electronic supplementary material is available online at https://dx.doi.org/10.6084/m9.figshare.c.4265774.

THE ROYAL SOCIETY PUBLISHING

Temperature-mediated inhibition of a bumblebee parasite by an intestinal symbiont

Evan C. Palmer-Young[1], Thomas R. Raffel[2] and Quinn S. McFrederick[1]

[1]Department of Entomology, University of California Riverside, Riverside, CA, USA
[2]Department of Biological Sciences, Oakland University, Rochester, MI, USA

ECP-Y, 0000-0002-9258-2073

Competition between organisms is often mediated by environmental factors, including temperature. In animal intestines, nonpathogenic symbionts compete physically and chemically against pathogens, with consequences for host infection. We used metabolic theory-based models to characterize differential responses to temperature of a bacterial symbiont and a co-occurring trypanosomatid parasite of bumblebees, which regulate body temperature during flight and incubation. We hypothesized that inhibition of parasites by bacterial symbionts would increase with temperature, due to symbionts having higher optimal growth temperatures than parasites. We found that a temperature increase over the range measured in bumblebee colonies would favour symbionts over parasites. As predicted by our hypothesis, symbionts reduced the optimal growth temperature for parasites, both in direct competition and when parasites were exposed to symbiont spent medium. Inhibitory effects of the symbiont increased with temperature, reflecting accelerated growth and acid production by symbionts. Our results indicate that high temperatures, whether due to host endothermy or environmental factors, can enhance the inhibitory effects of symbionts on parasites. Temperature-modulated manipulation of microbiota could be one explanation for fever- and heat-induced reductions of infection in animals, with consequences for diseases of medical and conservation concern.

1. Introduction

Temperature governs rates of the chemical interactions that underlie life, growth and reproduction, shaping biological processes from the level of the enzyme to the ecosystem [1]. One area of biology where temperature has demonstrated effects is on species interactions such as parasitism, where temperature can have profound effects on infection outcomes and transmission [2,3]. High host body temperatures have been shown to reduce infection intensity and infection-related mortality in both plants and animals [4–6], and metabolic and behavioural fevers are common responses to infection in vertebrates and insects [4,7,8].

Another factor that can influence infection outcome is the host-associated microbiota. The microbiota of the skin and gut constitute barriers to infection that can physically and chemically interfere with pathogen invasion, as well as modify host immune responses [9]. Because microbial taxa can differ widely in their optimal growth temperatures, alterations in temperature can affect the relative competitive abilities of co-occurring species [10]. These differential responses of interacting species to temperature, referred to variously as 'asymmetries' or 'mismatches' between the two species' thermal performance curves [11], can affect inhibitory interactions between symbionts and parasites [12]. This could have important consequences for the temperature dependence of infection. However, few studies have considered the effects of elevated

temperature on symbiotic microbiota [13,14], and the consequences of elevated temperature for gut parasite–symbiont competition remain unexplored.

Social bees present an ideal system in which to study effects of temperature on competition between symbionts and parasites. In this manuscript, we refer to core, apparently non-pathogenic members of the gut microbiota as 'symbionts', and to organisms with demonstrated negative effects on the host as 'parasites'. Both honeybees and bumblebees can be infected by a variety of parasites and pathogens, transmission of which is facilitated by the high density of hosts in colonies [15]. However, honeybees and especially bumblebees are facultative endotherms; they can maintain body and hive colony temperatures that are 30°C higher than that of the surrounding air [16,17]. This thermoregulatory capacity allows bumblebees to maintain the temperatures necessary for flight and brood development during times of year when other insects are inactive [18]. The elevated temperatures of bees facilitate not only foraging and colony development, but also defence against infection. In honeybees, high temperatures decreased infection with *Ascosphaera apis* (34°C [19]), deformed wing virus (33°C [20]), *Varroa* mites (45°C [21]), and *Nosema apis* and *N. ceranae* (37°C [22]).

In addition to their own parasite resistance mechanisms (including thermoregulation), honeybees and bumblebees have a well-characterized microbiota with demonstrated benefits against infection in larvae and adults [23]. The core gut microbiota consists of five main clades that are found in corbiculate ('pollen-basket') bees throughout the world [24]. The bumblebee microbiota is dominated by just three of these five core taxa—*Snodgrassella*, *Gilliamella* and *Lactobacillus* Firmicutes-5 ('Firm-5')—which together often account for over 80% of the total gut microbiota of worker bumblebees [25–27]. Bacteria isolated from the bumblebee gut had *in vitro* inhibitory activity against several bee pathogens [28], and microbiota rich in *Gilliamella* and *Lactobacillus* Firm-5 have been negatively correlated with trypanosomatid infection in bumblebees [25,27,29].

All of the core bumblebee gut symbionts have optimal incubation temperatures of 35–37°C [30]. In contrast, widespread trypanosomatid and microsporidian gut parasites (*Crithidia*, *Lotmaria* and *Nosema* spp.) have optimal temperatures of 25–27°C [31–33]. This difference in standard *in vitro* growth temperatures suggests that temperatures above the parasites' thermal optima will favour core symbionts over gut pathogens, due to differences in symbiont versus pathogen growth rates at these temperatures. However, no study has empirically quantified differences in the thermal performance curves (i.e. the relationship between temperature and growth rate) for symbionts versus parasites, or the temperature dependence of symbiont-mediated parasite inhibition, both of which are likely to shape the effects of temperature on infection in bumblebees.

We used a bumblebee-associated trypanosomatid gut parasite (*Crithidia bombi*) and a bacterial gut symbiont (*Lactobacillus bombicola*) of bumblebees to examine the temperature dependence of bee parasite–symbiont interactions *in vitro*. *Crithidia bombi* is a parasitic intestinal trypanosomatid that is both widespread and abundant in bumblebees [34,35]. This parasite reduces foraging efficiency and starvation tolerance in worker bees, growth rates and reproductive output of colonies, and post-hibernation survival and colony-founding in queens [36]. Its introduction has been correlated with decline of native bumblebees in South America [37], and its relative *Lotmaria passim* (formerly reported as *C. mellificae*) has been correlated with colony collapse in honeybees [38,39]. *Lactobacillus bombicola*, the most widely distributed bacterium found in a cross-species survey of bumblebees [28], is a member of the *Lactobacillus* Firm-5 clade. This clade of presumed mutualists is found in honeybees, bumblebees and other corbiculate bees worldwide [24]. In honeybees, Firm-5 was the clade with the strongest effect on gut metabolomics [40]. The abundance of Firm-5 bacteria has been negatively correlated with infection success of *C. bombi* [25,27].

The standard culturing temperatures for *C. bombi* and related trypanosomatids (27°C for *C. bombi* [31], 25°C for *L. passim* [32]) are lower than those used for *L. bombicola* and other Firm-5 bacteria (37°C [41]). This difference suggests different thermal optima in these two species, which could result in temperature-dependent competition that favours the symbiont *L. bombicola* over the parasite *C. bombi* at high temperatures. However, the quantitative temperature dependence of growth in these two species remains undescribed, and the effects of temperature on competition between the symbiont and the parasite remain unknown.

We measured *in vitro* growth of *C. bombi* and *L. bombicola* grown alone, together and sequentially across a range of incubation temperatures. We tested whether:

(1) *Crithidia bombi* and *L. bombicola* growth rates have differential responses to temperature, using metabolic-theory derived models to describe their thermal performance curves;
(2) competitive effects of *L. bombicola* on *C. bombi* increase with temperature and decrease the temperature of peak parasite growth, as predicted based on asymmetries in symbiont versus parasite thermal performance curves; and
(3) temperature-dependent chemical alterations to the growth environment made by *L. bombicola* are sufficient to explain temperature-dependent parasite inhibition.

2. Material and methods

(a) Overview of experiments

Three series of experiments were conducted to determine the temperature dependence of interactions between *C. bombi* and *L. bombicola*. (1) To estimate thermal performance curves, we measured each species's growth rate across a 25°C range of incubation temperatures. (2) To assess temperature dependence of direct competition, we cocultured *L. bombicola* with *C. bombi* at three temperatures ('coculture experiment'). (3) To assess whether a chemical mechanism could explain the temperature-dependent inhibition of parasites in coculture, we compared the effects of *L. bombicola* spent medium from different temperatures on *C. bombi* growth ('spent medium experiment'). The following text summarizes the methods. For details, see electronic supplementary material, Supplementary Methods.

(b) Cell cultures

Crithidia bombi cell cultures 'C1.1', 'IL13.2', 'S08.1' and 'VT1' were isolated from wild infected *Bombus terrestris* and *B. impatiens* by flow cytometry [31] (see electronic supplementary material, Supplementary Methods). Cultures were grown in 25 cm^2 culture flasks in 'FPFB' culture medium with 10% heat-inactivated fetal

bovine serum and incubated at 27°C for several weeks during the isolation process, then cryopreserved at −80°C until several weeks before the experiments began [31]. *Lactobacillus bombicola* strain 70-3, isolated from *Bombus lapidarius* collected near Ghent, Belgium (isolate '28288T' [41]), was obtained from the German Collection of Microorganisms and Cell Cultures (DSMZ). *Lactobacillus bombicola* was grown from frozen stock in 2 ml screw-cap tubes in MRS broth (Research Products International, Mt. Prospect, IL) with 0.05% cysteine (hereafter 'MRSC') and incubated at 27°C for several weeks before the experiment began.

(c) Thermal performance curves

Growth of each species was measured concurrently at six temperatures (17–42°C in 5°C increments) by optical density (OD 630 nm) in 96-well plates (*C. bombi*) or 2 ml tubes (*L. bombicola*) (see electronic supplementary material, Supplementary Methods). The entire experiment was repeated five (*C. bombi*, all strains) or six (*L. bombicola)* times, with each of six incubators assigned to a different temperature treatment during each repetition. We used metabolic theory equations to model the relationship between temperature and maximum specific growth rate, as calculated by a model-free spline fit (R package 'grofit' [42]) to the curve of log-transformed OD ($\ln(OD_t/OD_{t0})$) with respect to time [43]. A separate spline was fit to each replicate combination of incubator, strain and incubation temperature to estimate the maximum specific growth rate.

Thermal performance curves were modelled for each species and strain using the log-transformed Sharpe–Schoolfield equation [44,45], with temperature as the predictor variable and ln(maximum specific growth rate) as the response variable (equation (2.1)).

$$\ln(\text{rate}) = \ln(c) + E\left(\frac{1}{T_c} - \frac{1}{kT}\right) - \ln(1 + e^{E_h((1/kT_h)-(1/kT))}). \quad (2.1)$$

In equation (2.1), rate is the maximum specific growth rate; $\ln(c)$ is the natural log of the growth rate (in h^{-1}) at an arbitrary calibration temperature; E is the activation energy (in eV), which is proportional to the slope of the log-transformed thermal performance curve below the temperature of peak growth; T_c is the calibration temperature (in kelvin); k is Boltzmann's constant (8.62×10^{-5} eV K^{-1}); T is the incubation temperature (in kelvin); E_h is the high-temperature deactivation energy (in eV), which corresponds to the rate at which growth decreases at supraoptimal temperatures; and T_h is the supraoptimal temperature (in kelvin) at which growth rate is reduced by 50% relative to peak growth rate.

Solving equation (2.1) for the maximum growth rate yields the temperature of peak growth, T_{pk}, in kelvin [44]:

$$T_{pk} = \frac{E_h T_h}{E_h + kT_h \ln(E_h/E) - 1)}. \quad (2.2)$$

Model fit was optimized for each species and strain using nonlinear least squares with package *nls.multstart*, function 'nls_multstart' [46]. Model predictions with uncertainty estimates for T_{pk} and predicted growth at each temperature were estimated by bootstrap resampling (999 iterations). We constructed 95% bootstrap confidence intervals around the predictions of the original model using the 0.025 and 0.9725 quantiles of predictions from the bootstrap model fits.

(d) Coculture experiment

To assess the temperature dependence of direct competition, we cocultured *L. bombicola* with *C. bombi* strain VT1 at three incubation temperatures (27, 32 and 37°C). These temperatures were chosen for two reasons, one physiological and one statistical. Physiologically, this is a relevant temperature range for bumblebees. In the hive colony, thoracic temperatures of workers are generally 27–33°C (range 23–36°C), with brood (eggs, larvae and pupae) kept near 30°C [47]. During nest establishment, queens of *Bombus vosnesenskii* maintained even higher temperatures (37.4–38.8°C, day and night [47]). Statistically, 27–37°C is the temperature range over which the thermal performance curves of *L. bombicola* and *C. bombi* are differently or oppositely sloped (referred to by other authors as an 'asymmetry' between the two species' curves [48]). Growth rate of *L. bombicola* continues to increase, whereas growth rate of *C. bombi* plateaus and begins to decline.

Coculture experiments were conducted in 2 ml tubes in a mixed medium of 50% *Crithidia*-specific FPFB and 50% *Lactobacillus*-specific MRSC. Each experiment included three incubation temperatures crossed with two *C. bombi* start densities (initial OD = 0.010 and OD = 0.00 (cell free control)) and three *L. bombicola* start densities (initial OD = 0.010, 0.020 and cell free control; electronic supplementary material, figure S1). Growth measurements were made after 6 and 24 h of incubation. Growth rates of *L. bombicola* in monoculture were calculated using the 6 h measurement and the equation

$$r = \frac{\ln(OD_{t1}/OD_{t0})}{\Delta t},$$

where r represents relative growth rate (h^{-1}), OD_{t0} represents initial net OD of *L. bombicola*, OD_{t1} represents OD at the time of first measurement (6 h), and Δt is the amount of time between the start of the experiment and the first measurement. Growth rates of *C. bombi* in both monoculture and coculture were determined by haemocytometer cell counts, which allowed us to differentiate the larger *C. bombi* from *L. bombicola*. Initial cell density was estimated based on cell counts from tubes at time 0 h (OD = 0.010), averaged across all repetitions of the experiment. Final partial OD of *L. bombicola* was approximated by subtracting the estimated OD due to *C. bombi* from the total net OD, using a best-fit linear relationship between *C. bombi* cell density and OD. Growth rate of *L. bombicola* in coculture was approximated by subtracting the estimated *C. bombi* OD after 6 h of incubation from the total net OD (see electronic supplementary material, Supplementary Methods). Motility of *C. bombi* cells, which are mobile flagellates, was recorded during cell counts (see electronic supplementary material, Supplementary Methods).

Effects of temperature and *L. bombicola* start density on *C. bombi* growth rate were analysed by a general linear mixed model in R package lme4 [49] with experiment round as a random effect. *F*-tests were used to evaluate significance of model terms [50]; pairwise comparisons were made with R package 'lsmeans' [51]. Effects of temperature and *L. bombicola* start density on *C. bombi* cell motility were analysed by a bias-reduced binomial model [52] (see electronic supplementary material, Supplementary Methods). Cell motility was considered as a binary response variable (motility > 0). Likelihood ratio tests were used to evaluate significance of model terms. The relationship between *C. bombi* growth rate and *L. bombicola* OD after 24 h was tested by linear regression.

(e) Spent medium experiment

We used *L. bombicola* spent medium (i.e. cell-free supernatant of medium in which *L. bombicola* was grown for 20 h, then removed by filter sterilization) to test whether temperature-dependent inhibition observed in coculture experiments could be explained by temperature-dependent production of inhibitory chemicals by the symbiont. In the first stage of the experiment, *L. bombicola* spent medium was generated at different temperatures. In the second stage, growth of *C. bombi* (strain VT1) was measured in the presence of 50% spent medium at the same temperature at

which the spent medium was generated (electronic supplementary material, figure S2). Experiments used the same three incubation temperatures tested in the coculture experiment (27, 32 and 37°C) crossed with three *L. bombicola* start densities (OD of 0, 0.001 or 0.010). Each temperature treatment was replicated in two different incubators in each repetition of the experiment. The entire experiment was repeated three times, for a total of six incubator-level replicates.

Growth of *C. bombi* was measured in 96-well tissue culture plates in 50% MRSC-based spent medium and 50% *Crithidia*-specific FPFB medium. *Crithidia bombi* cell suspensions in *Crithidia*-specific FPFB medium [31] were added to an equal volume of spent medium for an initial net OD of 0.010, with 12 replicate wells per plate. Plates were incubated at the same temperature used for generation of the spent medium. Relative growth rate was computed using the 20 h OD measurement as in equation (2.1) above.

Effects of temperature and *L. bombicola* start density on *C. bombi* growth rate were analysed by a general linear mixed model with experiment round as a random effect [49]. *F*-tests were used to evaluate the significance of model terms [50]. Relationships between spent medium OD before filtration and temperature, spent medium pH and temperature, *C. bombi* growth rate and spent medium OD before filtration, and *C. bombi* growth rate and spent medium pH were tested by linear regression.

3. Results

Thermal performance curves showed higher temperatures of peak growth and upper limits of thermotolerance in *L. bombicola* than in *C. bombi* (figure 1). All *C. bombi* strains showed similar model-predicted peak growth temperatures (T_{pk}), ranging from 33.9°C in strain S08.1 (95% CI: 32.5–34.9°C) to 34.4°C in strain IL13.2 (95% CI: 32.9–35.3°C). These estimates were at least 5°C lower than the estimated T_{pk} for *L. bombicola* (39.8°C, 95% CI: 37.8–46.5°C; figure 1). For all strains of *C. bombi*, the temperature that inhibited growth by 50% (T_h) was below 38°C, or at least 5°C lower than the T_h for *L. bombicola* (figure 1; electronic supplementary material, table S1 for full model parameters). Due to the focus on higher temperatures, estimates of activation energy had high uncertainty, and overlapped both across *C. bombi* strains and between *C. bombi* and *L. bombicola*. For *C. bombi*, estimates ranged from 0.68 eV in strain IL13.2 (95% CI, 0.27–1.09) to 0.99 in strain VT1 (95% CI, 0.70–1.28), in comparison with 0.94 eV in *L. bombicola* (95% CI, 0.69–1.19, electronic supplementary material, table S1). These estimates are within the range compiled by previous authors in cross-taxon analyses, where 88% of activation energies lay between 0.2 and 1.2 eV [53]. The enzyme kinetics-based model imperfectly described the temperature dependence of *C. bombi* growth. Relative to empirically observed growth rates, fitted models consistently underestimated growth rates at 27°C and overestimated rates at 32°C (figure 1*b*). Further investigation, including study of the molecular and ecological drivers of growth rate, would be needed to clarify why parasite growth rates differ from metabolic theory-based model predictions at these temperatures.

Coculture with *L. bombicola* inhibited *C. bombi* growth and motility, and reduced temperature of peak *C. bombi* growth (figure 2). Growth rate of *C. bombi* was reduced by over 50% in coculture (model-predicted mean at 32°C: 0.66 ± 0.005 s.e. in monoculture versus 0.32 ± 0.005 s.e. in coculture,

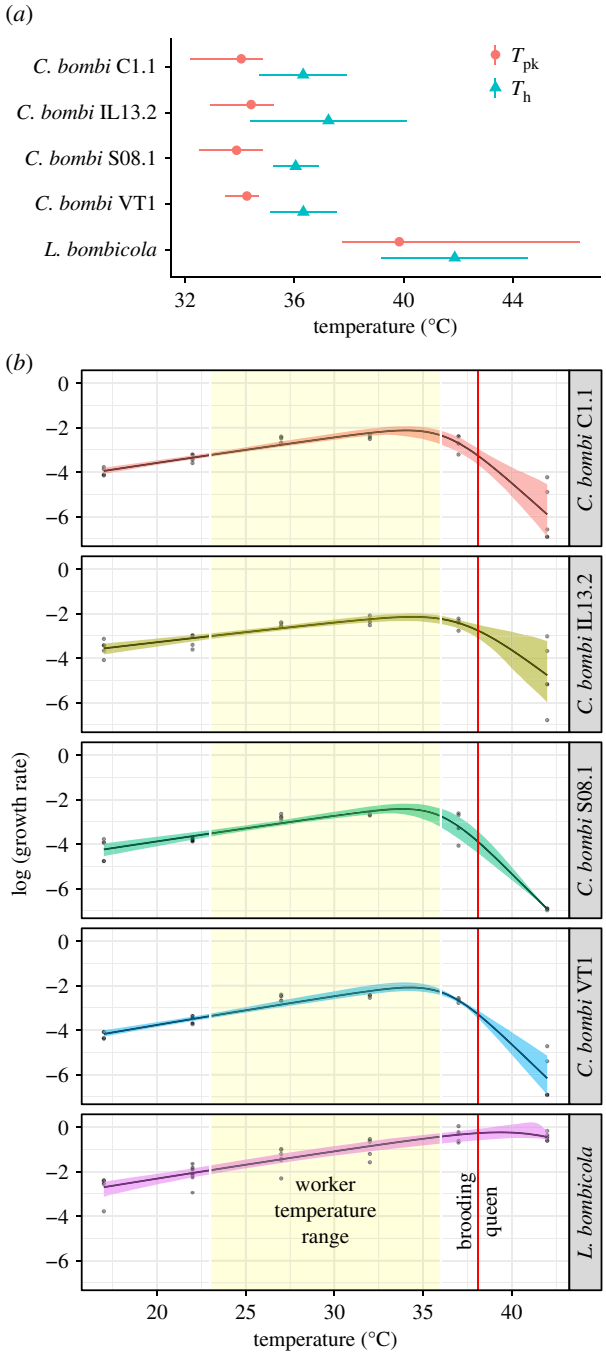

Figure 1. *Lactobacillus bombicola* exhibited higher peak growth temperature and greater tolerance to high temperatures than did *C. bombi*. (*a*) Model parameters for four *C. bombi* strains and *L. bombicola*. Points and error bars show means and 95% confidence intervals for peak growth temperature (T_{pk}, based on predictions from Sharpe–Schoolfield model from 999 bootstrap samples) and temperature at which growth was reduced by 50% relative to peak growth (T_h, based on Sharpe–Schoolfield model fitted by nonlinear least squares). (*b*) Full thermal performance curves used to derive model parameters shown in (*a*). The *y*-axis shows log-transformed specific growth rate (μ (h^{-1})) based on spline fits. Points show raw data, with one point per replicate (incubator). Trendlines show predictions from Sharpe–Schoolfield models. Shaded bands show 95% bootstrap confidence intervals. The curves are overlain with physiologically relevant temperature ranges for bumblebee workers (yellow vertical region) and queens (red vertical line), using data from [47]. (Online version in colour.)

figure 2*a*). We found stronger inhibitory effects of *L. bombicola* at higher temperatures (temperature × *L. bombicola* start density interaction, $F_{4,\ 43} = 3.30$, $p = 0.019$). Competition with *L. bombicola* altered the shape of the *C. bombi* thermal

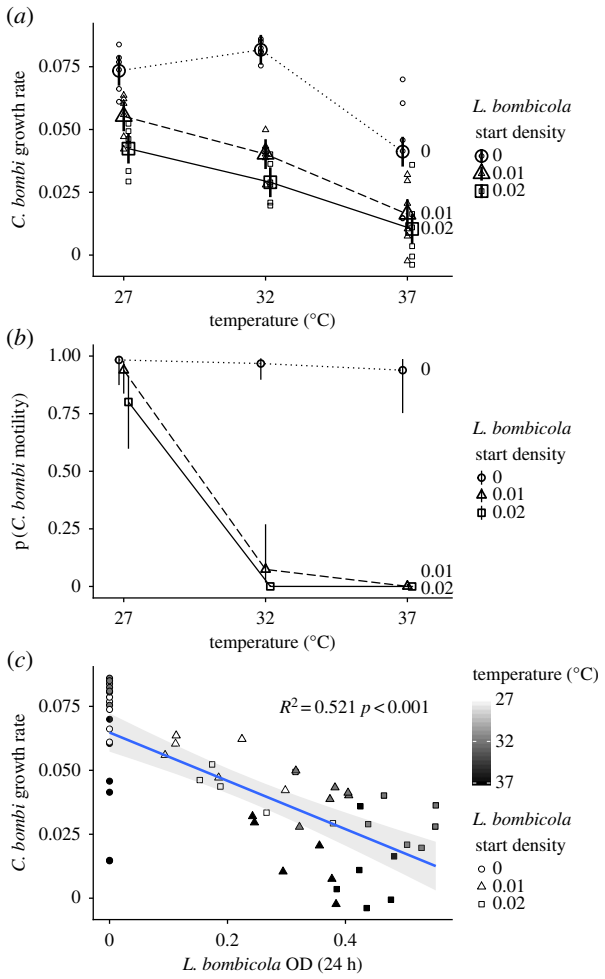

Figure 2. Competition with *L. bombicola* inhibited growth of *C. bombi* and reduced peak growth temperature, due to higher *L. bombicola* growth rates at high temperatures. (*a*) *Crithidia bombi* growth rate at three different temperatures in the presence of three starting optical densities (OD) of *L. bombicola*: 0 (i.e. no *L. bombicola*, hollow circles and dotted line), 0.01 (triangles and dashed line) and 0.02 (squares and solid line). Each small point represents specific growth rate (μ (h^{-1})) based on cell counts for a single incubator and repetition of the experiment. Large symbols and error bars show means and standard errors for each *L. bombicola* start density. Points have been offset by 0.5° to the left and right to reduce overplotting. (*b*) *Crithidia bombi* cell motility, observed microscopically after 24 h of coculture at the time of cell counts used to calculate growth rates in (*a*). Points and error bars indicate means and standard errors, and have been offset to the left and right to reduce overplotting. No movement of *C. bombi* was observed for any of the *C. bombi* cocultured with *L. bombicola* at 32 or 37°C. (*c*) *Crithidia bombi* growth rate was negatively correlated with OD of *L. bombicola* after 24 h of coculture. Partial OD of *L. bombicola* was estimated as net OD after subtraction of estimated OD due to *C. bombi*, based on correlation between OD and *C. bombi* cell concentration. Symbol fill indicates temperature; symbol shape indicates *L. bombicola* start density. Trendline shows linear model fit; shaded band shows 95% confidence interval. (Online version in colour.)

performance curve. Whereas *C. bombi* grew well throughout the range of 27–37°C in monoculture, growth was poor above 27°C in coculture (figure 2*a*). In addition to reducing growth, coculture with *L. bombicola* profoundly reduced *C. bombi* cell motility in a temperature-dependent fashion (temperature × *L. bombicola* interaction: $\chi^2_1 = 16.36$, $p < 0.001$, figure 2*b*). Whereas cells remained motile regardless of temperature in monoculture, no motility was observed above 27°C in coculture. The stronger effects of *L. bombicola* on *C. bombi* at high temperatures reflected increased *L. bombicola* cell densities, which were negatively correlated with *C. bombi* growth rate (estimate $= -0.094 \pm 0.013$ s.e., $t = -7.52$, $p < 0.001$, $R^2 = 0.521$).

Whereas *L. bombicola* had negative effects on *C. bombi*, *C. bombi* appeared to increase growth rate of *L. bombicola* under the conditions of our experiments. Estimated *L. bombicola* growth rate was nearly threefold higher in the presence of *C. bombi* than in its absence (temperature-adjusted mean growth rate $= 0.515 \pm 0.008$ s.e. with *C. bombi* versus 0.181 ± 0.008 s.e. without *C. bombi*, $t = 29.8$, $p < 0.001$; electronic supplementary material, figure S3).

Lactobacillus bombicola spent medium reduced *C. bombi* growth rate and peak growth temperature (figure 3). As in the coculture experiment, we found temperature-dependent inhibition of *C. bombi* by *L. bombicola* in the spent medium experiment. Whereas *C. bombi* grew well at all temperatures in control medium, growth was decreased at high temperatures in the presence of *L. bombicola* spent medium produced at high temperatures (temperature × *L. bombicola* start density interaction: $F_{4,43} = 8.28$, $p < 0.001$; figure 3*a*; electronic supplementary material, table S2). The temperature × *L. bombicola* start density interaction remained significant ($F_{4,42} = 10.57$, $p < 0.001$) after exclusion of one outlier (32°C, *L. bombicola* start density = 0.01), which had a standardized residual over threefold higher than that of any other data point. The stronger inhibitory effects of spent medium from higher temperatures reflected faster growth of *L. bombicola* at higher temperatures, which led to greater OD ($t = 3.56$, $p < 0.001$) and lower pH ($t = -3.84$, $p < 0.001$) achieved at higher temperatures during generation of the spent medium. As in the coculture experiment, *C. bombi* growth rate was negatively correlated with final OD of *L. bombicola* (estimate $= -0.083 \pm 0.017$ s.e., $t = -4.79$, $p < 0.001$, $R^2 = 0.29$; figure 3*b*), and even more strongly negatively correlated with acidity of spent medium (effect of pH: estimate $= 10.72 \pm 1.64$, $t = 6.54$, $p < 0.001$, $R^2 = 0.44$; figure 3*c*).

4. Discussion

As expected based on temperatures conventionally used in cell cultures, the symbiont *L. bombicola* had higher temperatures of peak growth and grew at higher temperatures than those tolerated by the parasite *C. bombi*. All four tested parasite strains exhibited similar thermal performance curves and inhibitory temperatures. This was somewhat surprising, given the documented among-strain variation in growth rate, infectivity, and ability to tolerate dessication, phytochemicals, antimicrobial peptides and gut microbiota [36,54]. The similarities between thermal performance profiles across strains could reflect strong stabilizing selection for enzymes and metabolic processes involved in thermotolerance, or adaptation to a consistent range of temperatures experienced in the bee abdomen. Regardless of the physiological underpinning, consistent upper limits of thermotolerance across parasite strains suggest that elevated temperature would be an effective defence against a range of *C. bombi* parasite genotypes.

The differently shaped thermal performance curves of *L. bombicola* and *C. bombi* indicate that a temperature increase over the range recorded in bumblebees would favour growth of symbionts over parasites, while the inhibitory effects of

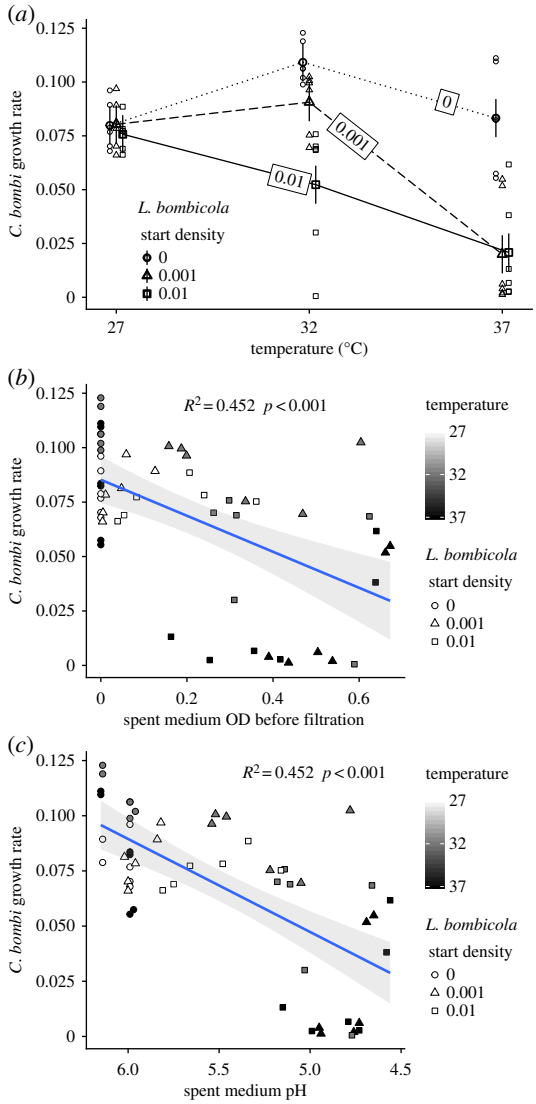

Figure 3. Spent medium from *L. bombicola* reduced growth rate and peak growth temperature of *C. bombi*, due to higher rates of *L. bombicola* growth and acid production at high temperatures. (*a*) *Crithidia bombi* growth rate at three different temperatures in the presence of spent medium. Spent medium was generated by growth of *L. bombicola* for 24 h from three starting densities: OD = 0 (i.e. no *L. bombicola*, hollow circles and dotted line), 0.001 (grey circles and dashed line) and 0.01 (black circles and solid line). Each small point represents specific growth rate (μ (h^{-1})) based on cell counts for a single incubator and repetition of the experiment. Large symbols and error bars show means and standard errors for each *L. bombicola* start density. Points have been offset by 0.5°C to the left and right to reduce overplotting. (*b*) *Crithidia bombi* growth rate was negatively correlated with OD of *L. bombicola* at the time when spent medium was filtered (i.e. after 24 h incubation). Symbol fill indicates temperature; symbol shape indicates *L. bombicola* start density. Note higher ODs achieved at higher temperatures, except in the *L. bombicola*-free controls (start density = 0, circles). Growth of *C. bombi* was assayed at the same temperature at which the spent medium had been generated. Trendline shows linear model fit, pooled across start densities and temperatures. Shaded band shows 95% confidence interval. (*c*) Growth rate of *C. bombi* was negatively correlated with acidity of *L. bombicola* spent medium. *X*-axis shows pH of spent medium after 20 h growth of *L. bombicola*, at the beginning of the *C. bombi* growth assay. As in (*b*), symbol fill indicates incubation temperature, symbol shape indicates *L. bombicola* start density, and trendline with shaded band shows linear model fit with 95% confidence bands. Note higher acidity (lower pH) achieved at higher temperatures, except in the *L. bombicola*-free controls (start density = 0, circles). (Online version in colour.)

L. bombicola on *C. bombi* indicate that this increased symbiont growth could constrain the ability of parasites to persist at high temperatures. Growth rates of *C. bombi* plateaued over the 27–33°C range found in bumblebee nests [47], and began to drop at the 38°C temperatures found in post-hibernation queens [47], the life stage at which bumblebees are most vulnerable to the effects of *C. bombi* [55]. In contrast, growth rate of *L. bombicola* continued to increase throughout this interval, rising nearly threefold between 27°C and 37°C. As a result, any effects of *L. bombicola* on *C. bombi* should become more pronounced at higher temperatures.

Within the gut, interactions between species may be positive, negative or neutral. For example, the bee gut symbionts *Snodgrassella* and *Gilliamella* facilitate one another's growth physically, via formation of multi-species biofilms [56], and chemically, via cross-feeding and modification of gut oxygen concentration and pH [40,57]. The effects of *L. bombicola* on *C. bombi* were strongly inhibitory. We have shown this inhibition to be chemically mediated by *L. bombicola*'s production of lactic acid, which was necessary and sufficient for inhibition of *C. bombi* growth [58]. Because *L. bombicola* rates of growth and acid production increased over the temperature range found in bees, we predict that increases in bee body temperature would reduce infection by increasing growth rate of *L. bombicola* and related Firm-5 bacteria, thereby decreasing gut pH to the point where parasites cannot grow. Thus, although parasites in monoculture are capable of growth throughout the range of temperatures found in bees, our results predict that competitive exclusion by symbionts could limit the parasite's thermal niche to cooler temperatures.

In contrast to the inhibitory effects of *L. bombicola* on *C. bombi*, *C. bombi* appeared to facilitate growth of *L. bombicola*. Given that *L. bombicola* did not grow at all in full-strength FPFB medium, this facilitation could reflect *C. bombi*'s catabolism of *L. bombicola*-inhibitory components in the mixed MRSC/FPFB growth medium. For example, FPFB medium contains 10% fetal bovine serum; complement proteins in mammalian serum can inhibit growth of bacteria [59]. Still, our findings indicate highly asymmetric competition between these two species, to the advantage of the symbiont.

The equilibrium outcome of competitive interactions depends on both interaction strengths and initial densities [60]. In the case of *L. bombicola* and *C. bombi*, initial symbiont densities had the strongest effects at intermediate temperatures typical of a bumblebee colony (27–33°C). At these moderate temperatures, lower symbiont and higher parasite growth rates might allow parasites to establish if initial symbiont densities are low. In contrast, at higher temperatures typical of those found in queens (greater than 37°C), high symbiont growth rates and direct high-temperature inhibition of parasites quickly made up for low initial symbiont density. In the social *Bombus* and *Apis* bees, core symbionts such as *Lactobacillus* Firm-5 are rapidly acquired by newly emerged bees from nest-mates and hive materials [26,61]. This socially mediated inoculation with core symbionts can establish a protective barrier against infection in colonies with microbiota that contain acid-producing *Gilliamella* and *Lactobacillus* Firm-5 [25,27]. However, symbiont-based defences might be weakened by treatment with antibiotics, which reduced populations of core gut symbionts and resistance to *C. bombi* [62]. Symbiont-based defences might also be relatively weak in solitary bees, which can be infected by the

same trypanosomatids that infect honeybees and bumblebees [32]. These bees lack a thermoregulated nest environment and a socially transmitted core gut microbiota, instead acquiring acidophilic gut symbionts from their environment [63]. As a result, solitary bees might be vulnerable to trypanosomatid infection during maturation of their gut microbiota, especially at cooler temperatures. However, no study has experimentally investigated trypanosomatid infections in solitary bee species, let alone the temperature dependence of such infection.

In our *in vitro* host–parasite–symbiont system, we found that high temperatures favoured symbionts over pathogens. This suggests that infection-related increases in body temperature, such as fever observed in honeybees [19], might allow hosts to clear pathogens while sparing beneficial symbionts. However, maintenance of elevated temperature comes at an energetic cost in both endothermic mammals and insects such as bumblebees [16,47]. In bees and other endothermic hosts, the ability to maintain parasite-inhibiting temperature will depend on sufficient caloric resources. Changing climates could result in phenological mismatch between queen emergence and floral blooms, and food shortages due to late-spring frosts [64]. Both phenomena could make queens vulnerable to parasites and threaten success of their colonies. Further study of temperature-dependent changes to microbiota and infection in live bees, and the effects of infection on endogenous thermoregulation and temperature preference, will be necessary to determine how our *in vitro* findings scale up to the organismal scale.

Studies of other host–symbiont–parasite systems are needed to determine whether high temperatures achieved during febrile states can be detrimental to symbiont populations [13], whether directly or via upregulation of host immunity [8,65], and the consequences of these effects for infection and host health. For example, short-term heat exposure altered soil microbial communities, and caused loss of the soil's activity against plant disease [66]. Numerous examples demonstrate that depletion of symbionts increases susceptibility to infection in animals as well [62,67]. Amid growing appreciation for the roles of temperature, fever, and the microbiome in infectious disease, understanding the effects of temperature on microbiota–parasite interactions may help to predict infection outcome in animals that exhibit fever, and in ectotherms that face infection in changing climates.

Data accessibility. All data are supplied in the electronic supplementary material, data S1.

Authors' contributions. E.C.P.-Y. and Q.S.M. conceived the study. E.C.P.-Y. and T.R.R. designed experiments. E.C.P.-Y. conducted experiments, analysed data and drafted the manuscript with guidance from T.R.R. and Q.S.M. All authors revised the manuscript and gave approval for publication.

Competing interests. The authors declare that they have no conflicts of interest.

Funding. This project was funded by a National Science Foundation Postdoctoral Research Fellowship to E.C.P.-Y. (NSF-DBI-1708945); USDA NIFA Hatch funds (CA-R-ENT-5109-H), NIH (5R01GM122060-02), and NSF MSB-ECA (1638728) to Q.S.M.; and an NSF-CAREER grant (IOS 1651888) to T.R.R. Funders had no role in study design, data collection and interpretation, or publication.

Acknowledgements. The authors thank the DSMZ for providing *L. bombicola*, Guang Xu and Ben Sadd for sharing DNA sequences, Daniel Padfield for sharing R script, and two anonymous reviewers for valuable comments that improved the initial submission.

References

1. Brown JH, Gillooly JF, Allen AP, Savage VM, West GB. 2004 Toward a metabolic theory of ecology. *Ecology* **85**, 1771–1789. (doi:10.1890/03-9000)
2. Raffel TR, Romansic JM, Halstead NT, McMahon TA, Venesky MD, Rohr JR. 2013 Disease and thermal acclimation in a more variable and unpredictable climate. *Nat. Clim. Change* **3**, 146–151. (doi:10.1038/nclimate1659)
3. Molnár PK, Sckrabulis JP, Altman KA, Raffel TR. 2017 Thermal performance curves and the metabolic theory of ecology—a practical guide to models and experiments for parasitologists. *J. Parasitol.* **103**, 423–439. (doi:10.1645/16-148)
4. Boorstein SM, Ewald PW. 1987 Costs and benefits of behavioral fever in *Melanoplus sanguinipes* infected by *Nosema acridophagus*. *Physiol. Zool.* **60**, 586–595. (doi:10.1086/physzool.60.5.30156132)
5. Wood GA. 1973 Application of heat therapy for the elimination of viruses from pip and stone fruit trees in New Zealand. *N. Z. J. Agric. Res.* **16**, 255–262. (doi:10.1080/00288233.1973.10421144)
6. Kluger MJ, Kozak W, Conn CA, Leon LR, Soszynski D. 1998 Role of fever in disease. *Ann. NY Acad. Sci.* **856**, 224–233. (doi:10.1111/j.1749-6632.1998.tb08329.x)
7. Kluger MJ, Vaughn LK. 1978 Fever and survival in rabbits infected with *Pasteurella multocida*. *J. Physiol.* **282**, 243–251. (doi:10.1113/jphysiol.1978.sp012460)
8. Boltaña S *et al.* 2013 Behavioural fever is a synergic signal amplifying the innate immune response. *Proc. R. Soc. B* **280**, 20131381. (doi:10.1098/rspb.2013.1381)
9. Bäumler AJ, Sperandio V. 2016 Interactions between the microbiota and pathogenic bacteria in the gut. *Nature* **535**, 85–93. (doi:10.1038/nature18849)
10. Bestion E, García-Carreras B, Schaum C-E, Pawar S, Yvon-Durocher G, Cameron D. 2018 Metabolic traits predict the effects of warming on phytoplankton competition. *Ecol. Lett.* **21**, 655–664. (doi:10.1111/ele.12932)
11. Cohen JM, Venesky MD, Sauer EL, Civitello DJ, McMahon TA, Roznik EA, Rohr JR. 2017 The thermal mismatch hypothesis explains host susceptibility to an emerging infectious disease. *Ecol. Lett.* **20**, 184–193. (doi:10.1111/ele.12720)
12. Daskin JH, Bell SC, Schwarzkopf L, Alford RA. 2014 Cool temperatures reduce antifungal activity of symbiotic bacteria of threatened amphibians—implications for disease management and patterns of decline. *PLoS ONE* **9**, e100378. (doi:10.1371/journal.pone.0100378)
13. Kikuchi Y, Tada A, Musolin DL, Hari N, Hosokawa T, Fujisaki K, Fukatsu T. 2016 Collapse of insect gut symbiosis under simulated climate change. *MBio* **7**, e01578-16. (doi:10.1128/mBio.01578-16)
14. Parkinson JF, Gobin B, Hughes WOH. 2014 Short-term heat stress results in diminution of bacterial symbionts but has little effect on life history in adult female citrus mealybugs. *Entomol. Exp. Appl.* **153**, 1–9. (doi:10.1111/eea.12222)
15. Evans JD, Spivak M. 2010 Socialized medicine: Individual and communal disease barriers in honey bees. *J. Invertebr. Pathol.* **103**, S62–S72. (doi:10.1016/j.jip.2009.06.019)
16. Esch H. 1960 Über die Körpertemperaturen und den Wärmehaushalt von *Apis mellifica*. *Z. Für Vgl. Physiol.* **43**, 305–335. (doi:10.1007/BF00298066)
17. Heinrich B. 1974 Thermoregulation in endothermic insects. *Science* **185**, 747–756. (doi:10.1126/science.185.4153.747)
18. Heinrich B. 2004 *Bumblebee economics: revised edition*. Cambridge, MA: Harvard University Press.
19. Starks PT, Blackie CA, Seeley TD. 2000 Fever in honeybee colonies. *Naturwissenschaften* **87**, 229–231. (doi:10.1007/s001140050709)
20. Di Prisco G, Zhang X, Pennacchio F, Caprio E, Li J, Evans JD, DeGrandi-Hoffman G, Hamilton M, Chen YP. 2011 Dynamics of persistent and acute deformed wing virus infections in honey bees, *Apis*

mellifera. *Viruses* **3**, 2425–2441. (doi:10.3390/v3122425)

21. Garedew A, Schmolz E, Lamprecht I. 2003 Microcalorimetric and respirometric investigation of the effect of temperature on the antivarroa action of the natural bee product-propolis. *Thermochim. Acta* **399**, 171–180. (doi:10.1016/S0040-6031(02)00453-7)
22. Martín-Hernández R, Meana A, García-Palencia P, Marín P, Botías C, Garrido-Bailón E, Barrios L, Higes M. 2009 Effect of temperature on the biotic potential of honeybee microsporidia. *Appl. Environ. Microbiol.* **75**, 2554–2557. (doi:10.1128/AEM.02908-08)
23. Raymann K, Moran NA. 2018 The role of the gut microbiome in health and disease of adult honey bee workers. *Curr. Opin. Insect Sci.* **26**, 97–104. (doi:10.1016/j.cois.2018.02.012)
24. Kwong WK, Medina LA, Koch H, Sing K-W, Soh EJY, Ascher JS, Jaffé R, Moran NA. 2017 Dynamic microbiome evolution in social bees. *Sci. Adv.* **3**, e1600513. (doi:10.1126/sciadv.1600513)
25. Koch H, Schmid-Hempel P. 2012 Gut microbiota instead of host genotype drive the specificity in the interaction of a natural host–parasite system. *Ecol. Lett.* **15**, 1095–1103. (doi:10.1111/j.1461-0248.2012.01831.x)
26. Billiet A, Meeus I, Van Nieuwerburgh F, Deforce D, Wäckers F, Smagghe G. 2017 Colony contact contributes to the diversity of gut bacteria in bumblebees (*Bombus terrestris*). *Insect Sci.* **24**, 270–277. (doi:10.1111/1744-7917.12284)
27. Mockler BK, Kwong WK, Moran NA, Koch H. 2018 Microbiome structure influences infection by the parasite *Crithidia bombi* in bumble bees. *Appl. Environ. Microbiol.* **84**, e02335-17. (doi:10.1128/AEM.02335-17)
28. Praet J, Parmentier A, Schmid-Hempel R, Meeus I, Smagghe G, Vandamme P. 2018 Large-scale cultivation of the bumblebee gut microbiota reveals an underestimated bacterial species diversity capable of pathogen inhibition. *Environ. Microbiol.* **20**, 214–227. (doi:10.1111/1462-2920.13973)
29. Koch H, Cisarovsky G, Schmid-Hempel P. 2012 Ecological effects on gut bacterial communities in wild bumblebee colonies. *J. Anim. Ecol.* **81**, 1202–1210. (doi:10.1111/j.1365-2656.2012.02004.x)
30. Engel P, James RR, Koga R, Kwong WK, McFrederick QS, Moran NA. 2013 Standard methods for research on *Apis mellifera* gut symbionts. *J. Apic. Res.* **52**, 1–24. (doi:10.3896/IBRA.1.52.4.07)
31. Salathé R, Tognazzo M, Schmid-Hempel R, Schmid-Hempel P. 2012 Probing mixed-genotype infections I: extraction and cloning of infections from hosts of the trypanosomatid *Crithidia bombi*. *PLoS ONE* **7**, e49046. (doi:10.1371/journal.pone.0049046)
32. Schwarz RS, Bauchan GR, Murphy CA, Ravoet J, de Graaf DC, Evans JD. 2015 Characterization of two species of Trypanosomatidae from the honey bee *Apis mellifera*: *Crithidia mellificae* Langridge and McGhee, and *Lotmaria passim* n. gen., n. sp. *J. Eukaryot. Microbiol.* **62**, 567–583. (doi:10.1111/jeu.12209)
33. Gisder S, Möckel N, Linde A, Genersch E. 2011 A cell culture model for *Nosema ceranae* and *Nosema apis* allows new insights into the life cycle of these important honey bee-pathogenic microsporidia. *Environ. Microbiol.* **13**, 404–413. (doi:10.1111/j.1462-2920.2010.02346.x)
34. Schmid-Hempel R, Tognazzo M. 2010 Molecular divergence defines two distinct lineages of *Crithidia bombi* (Trypanosomatidae), parasites of bumblebees. *J. Eukaryot. Microbiol.* **57**, 337–345. (doi:10.1111/j.1550-7408.2010.00480.x)
35. Schmid-Hempel P. 2001 On the evolutionary ecology of host–parasite interactions: addressing the question with regard to bumblebees and their parasites. *Naturwissenschaften* **88**, 147–158. (doi:10.1007/s001140100222)
36. Sadd BM, Barribeau SM. 2013 Heterogeneity in infection outcome: lessons from a bumblebee–trypanosome system. *Parasite Immunol.* **35**, 339–349. (doi:10.1111/pim.12043)
37. Schmid-Hempel R *et al*. 2014 The invasion of southern South America by imported bumblebees and associated parasites. *J. Anim. Ecol.* **83**, 823–837. (doi:10.1111/1365-2656.12185)
38. Cornman RS, Tarpy DR, Chen Y, Jeffreys L, Lopez D, Pettis JS, vanEngelsdorp D, Evans JD. 2012 Pathogen webs in collapsing honey bee colonies. *PLoS ONE* **7**, e43562. (doi:10.1371/journal.pone.0043562)
39. Ravoet J, Maharramov J, Meeus I, De Smet L, Wenseleers T, Smagghe G, de Graaf DC. 2013 Comprehensive bee pathogen screening in Belgium reveals *Crithidia mellificae* as a new contributory factor to winter mortality. *PLoS ONE* **8**, e72443. (doi:10.1371/journal.pone.0072443)
40. Kešnerová L, Mars RAT, Ellegaard KM, Troilo M, Sauer U, Engel P. 2017 Disentangling metabolic functions of bacteria in the honey bee gut. *PLoS Biol.* **15**, e2003467. (doi:10.1371/journal.pbio.2003467)
41. Praet J, Meeus I, Cnockaert M, Houf K, Smagghe G, Vandamme P. 2015 Novel lactic acid bacteria isolated from the bumble bee gut: *Convivina intestini* gen. nov., sp. nov., *Lactobacillus bombicola* sp. nov., and *Weissella bombi* sp. nov. *Antonie Van Leeuwenhoek* **107**, 1337–1349. (doi:10.1007/s10482-015-0429-z)
42. Kahm M, Hasenbrink G, Lichtenberg-Fraté H, Ludwig J, Kschischo M. 2010 grofit: fitting biological growth curves with R. *J. Stat. Softw.* **33**, 1–21. (doi:10.18637/jss.v033.i07)
43. Hasenbrink G, Kolacna L, Ludwig J, Sychrova H, Kschischo M, Lichtenberg-Fraté H. 2007 Ring test assessment of the mKir2.1 growth based assay in *Saccharomyces cerevisiae* using parametric models and model-free fits. *Appl. Microbiol. Biotechnol.* **73**, 1212–1221. (doi:10.1007/s00253-006-0589-x)
44. Padfield D, Yvon-Durocher G, Buckling A, Jennings S, Yvon-Durocher G. 2015 Rapid evolution of metabolic traits explains thermal adaptation in phytoplankton. *Ecol. Lett.* **19**, 133–142. (doi:10.1111/ele.12545)
45. Schoolfield RM, Sharpe PJH, Magnuson CE. 1981 Non-linear regression of biological temperature-dependent rate models based on absolute reaction-rate theory. *J. Theor. Biol.* **88**, 719–731. (doi:10.1016/0022-5193(81)90246-0)
46. Padfield D, Matheson G. 2018 R package nls.multstart: robust non-linear regression using AIC scores. See https://cran.r-project.org/web/packages/nls.multstart/index.html.
47. Heinrich B. 1972 Patterns of endothermy in bumblebee queens, drones and workers. *J. Comp. Physiol.* **77**, 65–79. (doi:10.1007/BF00696520)
48. Dell AI, Pawar S, Savage VM. 2014 Temperature dependence of trophic interactions are driven by asymmetry of species responses and foraging strategy. *J. Anim. Ecol.* **83**, 70–84. (doi:10.1111/1365-2656.12081)
49. Bates D, Mächler M, Bolker B, Walker S. 2015 Fitting linear mixed-effects models using lme4. *J. Stat. Softw.* **67**, 1–48. (doi:10.18637/jss.v067.i01)
50. Fox J, Weisberg S. 2011 *An R companion to applied regression*, 2nd edn. Thousand Oaks, CA: Sage. See http://socserv.socsci.mcmaster.ca/jfox/Books/Companion.
51. Lenth RV. 2016 Least-squares means: the R package lsmeans. *J. Stat. Softw.* **69**, 1–33. (doi:10.18637/jss.v069.i01)
52. Kosmidis I. 2013 R package brglm: bias reduction in binary-response generalized linear models. See http://www.ucl.ac.uk/ucakiko/software.html.
53. Dell AI, Pawar S, Savage VM. 2011 Systematic variation in the temperature dependence of physiological and ecological traits. *Proc. Natl Acad. Sci. USA* **108**, 10 591–10 596. (doi:10.1073/pnas.1015178108)
54. Palmer-Young EC, Sadd BM, Stevenson PC, Irwin RE, Adler LS. 2016 Bumble bee parasite strains vary in resistance to phytochemicals. *Sci. Rep.* **6**, 37087. (doi:10.1038/srep37087)
55. Brown MJF, Schmid-Hempel R, Schmid-Hempel P. 2003 Strong context-dependent virulence in a host–parasite system: reconciling genetic evidence with theory. *J. Anim. Ecol.* **72**, 994–1002. (doi:10.1046/j.1365-2656.2003.00770.x)
56. Engel P, Martinson VG, Moran NA. 2012 Functional diversity within the simple gut microbiota of the honey bee. *Proc. Natl Acad. Sci. USA* **109**, 11 002–11 007. (doi:10.1073/pnas.1202970109)
57. Zheng H, Powell JE, Steele MI, Dietrich C, Moran NA. 2017 Honeybee gut microbiota promotes host weight gain via bacterial metabolism and hormonal signaling. *Proc. Natl Acad. Sci. USA* **114**, 4775–4780. (doi:10.1073/pnas.1701819114)
58. Palmer-Young EC, Raffel TR, McFrederick QS. 2018 pH-mediated inhibition of a bumble bee parasite by an intestinal symbiont. *bioRxiv*, 336347. (doi:10.1101/336347)
59. Rowley D, Wardlaw AC. 1958 Lysis of gram-negative bacteria by serum. *Microbiology* **18**, 529–533.
60. Volterra V. 1928 Variations and fluctuations of the number of individuals in animal species living together. *ICES J. Mar. Sci.* **3**, 3–51. (doi:10.1093/icesjms/3.1.3)

61. Powell JE, Martinson VG, Urban-Mead K, Moran NA. 2014 Routes of acquisition of the gut microbiota of the honey bee *Apis mellifera*. *Appl. Environ. Microbiol.* **80**, 7378–7387. (doi:10.1128/AEM.01861-14)
62. Koch H, Schmid-Hempel P. 2011 Socially transmitted gut microbiota protect bumble bees against an intestinal parasite. *Proc. Natl Acad. Sci. USA* **108**, 19 288–19 292. (doi:10.1073/pnas.1110474108)
63. McFrederick QS, Wcislo WT, Taylor DR, Ishak HD, Dowd SE, Mueller UG. 2012 Environment or kin: whence do bees obtain acidophilic bacteria? *Mol. Ecol.* **21**, 1754–1768. (doi:10.1111/j.1365-294X.2012.05496.x)
64. Ogilvie JE, Griffin SR, Gezon ZJ, Inouye BD, Underwood N, Inouye DW, Irwin RE. 2017 Interannual bumble bee abundance is driven by indirect climate effects on floral resource phenology. *Ecol. Lett.* **20**, 1507–1515. (doi:10.1111/ele.12854)
65. Xu J, James RR. 2012 Temperature stress affects the expression of immune response genes in the alfalfa leafcutting bee, *Megachile rotundata*. *Insect Mol. Biol.* **21**, 269–280. (doi:10.1111/j.1365-2583.2012.01133.x)
66. van der Voort M, Kempenaar M, van Driel M, Raaijmakers JM, Mendes R. 2016 Impact of soil heat on reassembly of bacterial communities in the rhizosphere microbiome and plant disease suppression. *Ecol. Lett.* **19**, 375–382. (doi:10.1111/ele.12567)
67. Raymann K, Shaffer Z, Moran NA. 2017 Antibiotic exposure perturbs the gut microbiota and elevates mortality in honeybees. *PLoS Biol.* **15**, e2001861. (doi:10.1371/journal.pbio.2001861)